Dense MgB$_2$ Ceramics by Ultrahigh Pressure Field-Assisted Sintering

Mythili Prakasam [1],*, Felix Balima [1], Jacques Noudem [2] and Alain Largeteau [1]

[1] CNRS, University Bordeaux, ICMCB, UMR 5026, 33600 Pessac, France; balima.felix@gmail.com (F.B.); alain.largeteau@u-bordeaux.fr (A.L.)

[2] Normandie University, Ensicaen, Unicaen, CNRS, CRISMAT, 14000 Caen, France; jacques.noudem@ensicaen.fr

* Correspondence: mythili.prakasam@icmcb.cnrs.fr; Tel.: +33-54000-8435

Abstract: Magnesium diboride (MgB$_2$) ceramics, due to their impressive transition temperature of 39 K for superconductivity, have been widely investigated. The possibility to obtain highly dense MgB$_2$ ceramics with fine microstructure and grain boundaries acting as pinning sites by novel high-pressure-assisted spark plasma sintering (HP-SPS) is reported in this article. HP-SPS was employed to reach 100% density in MgB$_2$ ceramics, and high pressure was utilized in the consolidation of MgB$_2$. An increase in pressure helped in stabilizing the MgB$_2$ phase above thermal decomposition, thus avoiding the formation of non-superconducting phases such as MgO and MgB$_4$. Pressure allowed strengthening of the covalent bond (condensation effect) to increase the thermal stability of MgB$_2$. HP-SPS yielded high mechanical hardness in MgB$_2$ (1488 HV). For better electrical connectivity, which leads to large magnetic moments in high density samples were obtained with the beneficial effect of high applied pressure (1.7–5 GPa) at high temperature (>1000 °C). The combination of the SPS process and high pressure ensured retention of the homogeneous fine microstructure required to obtain high current density and high hardness.

Keywords: MgB$_2$; high pressure; thermal stability; rapid sintering; superconductor

1. Introduction

Superconductors are materials whose conductivity tends to infinite as resistivity tends to zero at a critical temperature. Critical current density refers to a current density that is strong enough to quench the superconducting state. MgB$_2$ is one of the potential light materials with a medium critical temperature (T$_c$ = 39 K) for diverse applications requiring improvement of the superconducting properties. It has a high charge carrier density, 1.7–2.8 × 10^{23} A/cm^3, a high critical current density J$_c$ of about 107 A/cm^2 (4.2 K, 0 T), as well as high coherency lengths ξ$_{ab}$(0) = 37,120 Å and ξ$_c$(0) = 16–36 Å. MgB$_2$ can be used as an alternative to other low-temperature superconductors such as NbTi and Nb$_3$Sn. MgB$_2$ has a hexagonal crystal structure and is an intermetallic with simple stoichiometry [1,2]. The advantages of MgB$_2$ include its low cost, light weight, and high hardness. Progress in manufacturing technologies has led to obtaining MgB$_2$ as tapes, bulk, and in wire form, either through ex situ or in situ methods [3–7]. The ex situ method involves compaction of starting precursors of the MgB$_2$ phase (density = 2.62 g·cm^{-3}) at high temperature and high pressure, yielding a highly dense MgB$_2$ phase (above 95% relative density). Thus, the obtained MgB$_2$ phase is denser than in its in situ counterpart (80% relative density). Various research teams reported on employing recent techniques such as field-assisted sintering or high-pressure-assisted sintering techniques [8–12] to obtain MgB$_2$ dense compact samples with relative densities greater than 95%, in comparison with other conventional pressureless sintering techniques. The influence of the sintering parameters in field-assisted sintering,

such as pressure, dwell time, temperature, and heating/cooling rate, on the structural, microstructural, and superconducting properties of MgB_2 have been studied [8–12]. An increase in the relative density of MgB_2 up to 99% was achieved when the sintering temperatures were in the range of 900–1050 °C [5]. Appearance of MgO and MgB_4 phases in MgB_2 ceramics was observed by Habler et al. [11] when the sintering temperatures were increased above 950 °C. High pressure had a significant influence to increase relative density [3]. No significant effects on the sintering rate and dwell time in yielding dense MgB_2 compacts were reported. However, the role of the internal microstructure of the sintered compact influenced the trapped field performance through a combination of extrinsic (reduced volume fraction of the MgB_2 phase and presence of parasitic phases between the grains and particles) and intrinsic (local micro defects within the grains or between the particles) properties, which reduced the current density values of the superconductor.

The influence of pressure on the mechanical properties of hard and super-hard materials is well known. The combination of high-pressure and field-assisted sintering yields nanostructured ceramics, stabilizes thermosensitive phases, and facilitates early chemical reaction. Recently, there have been few reports on the possibility to combine a pulsed power source with a high-pressure toroidal-type apparatus reaching pressures up to 7.8 GPa and temperature of 1950 °C [13–16]. The objective of this work was to sinter MgB_2 fully dense ceramics by maintaining the microstructured grains and stabilize the initial MgB_2 phase by inhibiting the parasitic phases, such as MgO and MgB_4, that appear due to thermal decomposition. We hypothesized that by employing the beneficial effects of a field-assisted sintering direct current (DC) pulse current with high pressure, we would obtain dense MgB_2 ceramics at high pressure and at a temperature above the thermal decomposition of MgB_2. In our earlier work, we demonstrated the possibility to obtain materials such as SiC in comparison with conventional spark plasma sintering (SPS) with the help of high pressure [13]. The application of pressure (as a "driving force") manifests itself in different ways such as reduced sintering temperature leading to conservation of grain size and sintering the high-pressure structural phase of alumina [15]. Krinistina et al. [12] reported on obtaining dense MgB_2 samples by employing high-pressure deformation and annealing, which also resulted in obtaining nanostructured ceramics with increased critical current density in spite of the presence of MgO formed in the grain boundaries. Application of high pressure leads to increased critical current density, necessary for the superconducting properties of MgB_2 ceramics.

In the present work, we used our in-house built high-pressure SPS equipment [8–12], which enables a maximum pressure of 6 GPa and temperatures up to 1800 °C to be reached, given its versatility, for the synthesis and sintering of highly dense MgB_2 ceramics at low temperature. Our HP-SPS equipment, capable of reaching 3000 A for 10 V with a pulse of 3.3 ms, was employed by using the Belt system to generate a high pressure up to 6 GPa, but other possibilities such as the Bridgman system could also be employed [13]. High-pressure spark plasma sintering was used for sintering dense MgB_2 without additional parasitic oxide and magnesium boride phases for prospective applications as cryomagnets at 20 K. Conventional SPS was also used, as a reference at low pressure, to compare the influence of various sintering parameters on the MgB_2 ceramics. In the present work, the application of high pressure in HP-SPS does not permit voids; hence, vacuum nor air can enter the system, which can thus be considered as a closed system. In the case of conventional SPS, a static primary vacuum is used to avoid the destruction of the graphite mold. Further sintering in the presence of graphite causes a reducing atmosphere during sintering by conventional SPS and HP-SPS. In both conventional SPS and HP-SPS, the sample was in direct contact with the pulse current. The characterization and results of the experiments are discussed in the following sections.

2. Materials and Methods

High-pressure sintering experiments (using the HP-SPS-Belt equipment) and conventional SPS experiments were conducted in ICMCB (Bordeaux, France) to study the influences of pressure and pulse electric direct current on sintered compacts. The detailed experiment set up, temperature, and pressure calibration were described in our previous work [14]. For all experiments, the pressure was first

increased up to the desired value; then, the heating cycle was executed. The maximum temperature was maintained at a dwell time of 5 min. Decompression was done after cooling. The heating and cooling rates were maintained constant in all the sintering experiments. The high-pressure cells were contained in a graphite furnace with 17 mm internal diameter corresponding to the maximum sample diameter in our HP-SPS cell. The starting commercial MgB_2 powder was from PAVEZYUM, Advanced Chemicals (Istanbul, Turkey). Regarding the quality of the starting powder, the purity was 97%, with the traces of MgO (2%) and MgB_4 (0.1%), and powder particle size was 150 microns. Starting powder (2.5 g) was used in the high-pressure experiments. Since the sintered sample had a 17 mm diameter, it was in contact with the graphite furnace tube. However, in the HP-SPS Belt apparatus it was also possible to obtain a 10 mm diameter, with a pre-compacted pellet of the hexagonal boron nitride (h-BN) ring to obtain comparable sample sizes with conventional SPS for the 10 mm diameter die. The external diameter of the h-BN ring was 17 mm to match the graphite furnace. The sample was compressed with two graphite studs similar to the conventional SPS die assembly. The temperature was adjusted by modifying the percentage of the filling of the set pulses with elementary 3.3 ms pulses. At room temperature, cold isostatic pressure (CIP) experiments (200 MPa for 5 min) and HP-SPS Belt experiments (3 and 5 GPa for 5 min) were performed to compare the influence of pressure, independently of temperature, on raw powders of MgB_2 and on the appearance of any parasitic phases. High-pressure experiments were performed for 5 min in the temperature range from 850 to 1300 °C and pressures of 1.7, 3 and 5 GPa. For experiments by conventional SPS, 1 g of starting powder was filled into a graphite die having an inner diameter of 10 mm. The graphite die was covered with a thermal insulator carbon fiber. An optical pyrometer was used to measure the temperature of the graphite die surface. The graphite mold was placed in an SPS operating chamber (DR. SINTER LAB, Model SPS-515S), capable of reaching 1500 A for 10 V, and heating was provided by Thyristor, under vacuum at 10^{-3} Pa. The pulse (3.3 ms) sequence generated from the DC electric current for the SPS applied voltage on all the samples was 12:2 (i.e., 12 ON/2 OFF). These same parameters were also used for the HP-SPS Belt equipment, which allows the parameters studied to be comparable. A pressure of 100 MPa was applied for sintering. Densities of sintered samples were measured by the Archimedes method with distilled water as the reference liquid. The microstructure and compositional variation (by contrast) of the sintered samples was observed on the fractured surfaces by electron diffraction scattering (EDS) using a JEOL JSM 6700F operating at 15 kV. SEM and EDS images were used to estimate the grain size, grain morphology, and analyze the elements. Sintered samples were milled and characterized by powder X-ray diffraction (XRD). Powder X-ray diffraction (XRD) analysis was performed with a PANalytical X'pert MDP diffractometer with an h-h Bragg–Brentano configuration and a backscattering graphite monochromator for K_α Cu radiation working at 40 kV and 40 mA. Temperature-dependent XRD was performed using a powder diffractometer (PANalytical X'Pert Pro) equipped with a high-temperature chamber Anton Paar HTK16 (1600 °C) measuring K_α Cu radiation. The in situ XRD temperatures were analyzed from room temperature until 1400 °C. Hardness measurements of the MgB_2 ceramics were analyzed with a Shimadzu DUH-211S Vickers hardness indenter at 500 g of the load. The resistivity of the sintered samples was measured by the 4-point contact probe method.

3. Results and Discussion

From the literature review [1–12], it can be inferred that the thermal decomposition of MgB_2 starts around 830 °C. We performed conventional SPS experiments at 100 MPa with a dwell time of 5 min and observed that thermal decomposition appeared at 1050 °C. The shift of this thermal decomposition to a higher temperature can be attributed to the benefit of 100 MPa pressure under pulse electric current. We further observed by conventional SPS that when the applied pressure was increased, the crystallite size decreased at 950 °C, as shown below. HP-SPS experiments were conducted in the range 950–1300 °C. We observed it was possible to obtain 100% density at 950 °C and 5 GPa, but achieving full density at 3 GPa and at 1100 °C was not possible, even though no thermal decomposition was observed at 1100 °C by XRD, as shown below.

3.1. X-ray Diffraction and Density Analyses

In order to evaluate structural and phase transformations, MgB_2 was subjected to different analyses based on temperature and pressure. Figure 1a shows the temperature XRD in situ, where the peak at $43°$ is attributed to the main peak (101) of MgB_2. This in situ analysis shows a shoulder peak arising from the main peak at 650 °C, indicating the appearance of MgO, and traces of MgO likely appear at 600 °C. Though there are reports in the literature that thermal decomposition occurs at 830 °C, this variation can be assumed to arise from the starting precursor powders of MgB_2 used for study, mainly regarding the grain size, process for manufacturing this powder, and temperature for this process. There were some inevitable traces of MgO already present in the starting powder.
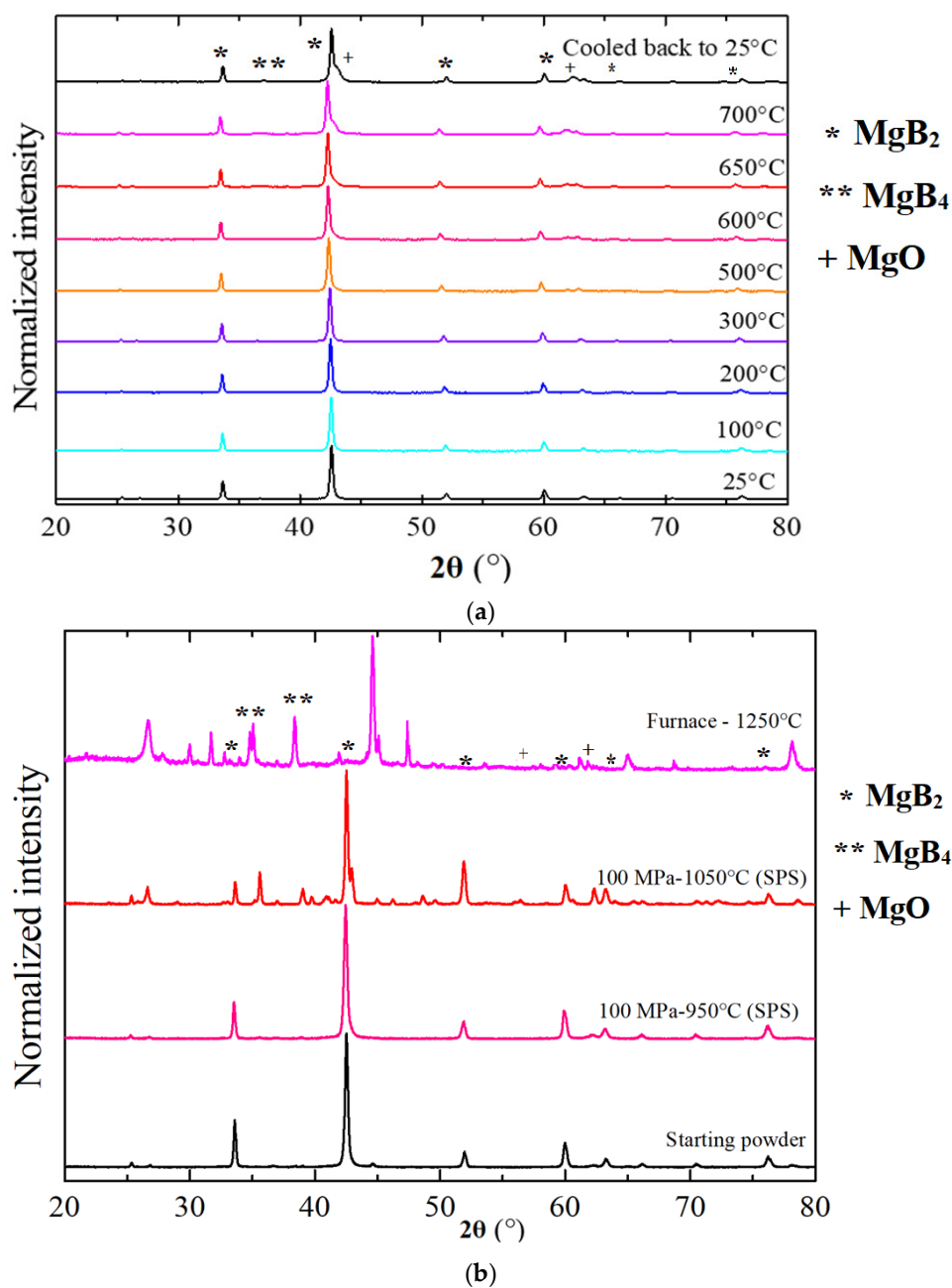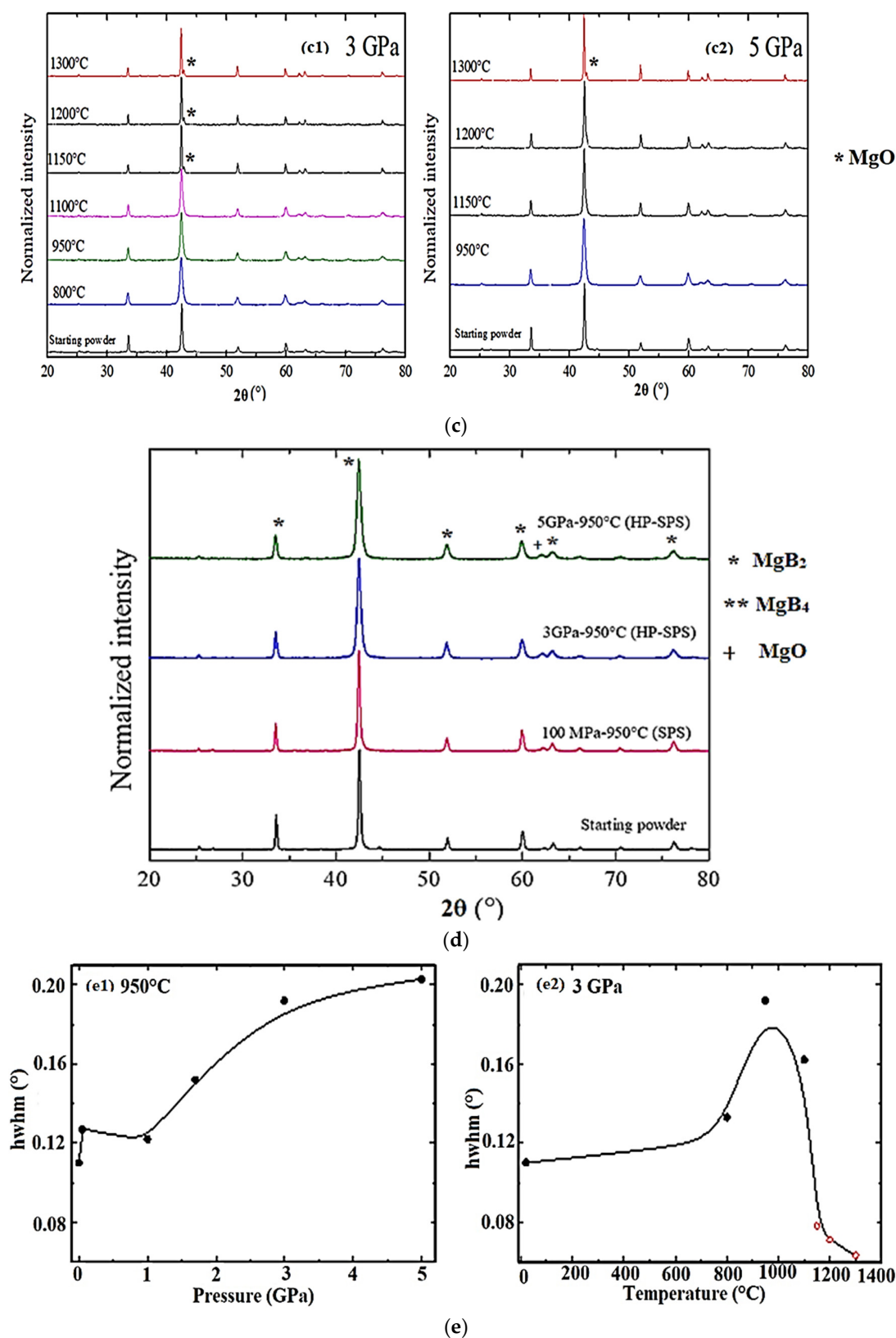

(a)

(b)

Figure 1. *Cont.*

Figure 1. (**a**) Phase stability of MgB$_2$ with temperature at ambient pressure by in situ XRD. (**b**) Phase stability of MgB$_2$ with temperature at 100 MPa and decomposition of MgB$_2$ at 1250 °C. (**c**) Phase stability of MgB$_2$ with temperature at (c1) 3 GPa and (c2) 5 GPa. (**d**) Phase stability of MgB$_2$ with pressure at 950 °C (**e**) Evolution of peak (101) width by XRD on MgB$_2$ with (e1) Pressure at 950 °C and (e2) Temperature at 3 GPa.

From Figure 1b, it can be observed that the percentage of parasitic phases such as MgO (inside the shoulder of the main peak) increased when the processing temperature increased. This can be due to the decomposition reaction of $2MgB_2 \rightarrow MgB_4 + Mg(g)$. The diffractogram at 1250 °C, 5 min at ambient pressure, shows the total decomposition of MgB_2 (Figure 1b). The thermal decomposition appears at 1050 °C under 100 MPa by conventional SPS, as shown in Figure 1b.

The behavior of MgB_2 under high pressure at 950 °C by conventional SPS was studied at 100 MPa (Figure 1c). To increase the density and Vickers hardness (HV) of the sintered compacts of MgB_2, a high temperature was employed. The evolution of MgB_2 at high temperatures at 3 GPa and 5 GPa was studied. Figure 1c shows, at 950 °C, the diffractograms for various pressures by conventional SPS and by HP-SPS; MgB_2 was thermally stable by the help of pressure, although thermal decomposition occurred around 650 °C at ambient pressure. It can be observed from Figure 1d that the parasitic peaks of MgO started to appear at 1150 °C and 1300 °C at 3 GPa and 5 GPa, respectively (shown with symbol *). These results clearly demonstrate that the increase in pressure induces an increase in the thermal stability domain of MgB_2.

We could infer, based on Figure 1, that pressure was highly beneficial to preserve the starting composition by increasing the thermal stability domain. Pressure allows the stabilization of covalent bonds under high-pressure conditions, leading to an increase in thermal stability of MgB_2 because the phases possessing lower specific volume are more stable under high pressure. We could hypothesize that the shrinkage of specific volume caused by high pressure was similar to the behavior of strengthening by covalent bonds. This phenomenon is similar to the condensation effect where shrinking, as opposed to expansion, is caused by an increase in temperature. The aforesaid high-pressure behavior and increase in thermal stability is in good accordance with previous work reported by Cannon, where he showed that the thermal stability of chemical elements increases with pressure when no polymorphic transformation exists [17,18].

From Figure 1e, it can be inferred that the crystallite size decreased with the increase in pressure at 950 °C (Table 1). This can be attributed to the fracturing of larger crystallites, from the starting powder, induced by the high pressure. Experiments by Rietveld at room temperature for different pressures, such as 200 MPa, 3, and 5 GPa, confirmed that the parasitic phases (MgO, MgB_4) appearing in the sintered samples was a result of the effect of temperature, but not high pressure, because all diffractograms were similar to the starting powder. Interestingly, under the influence of temperature, the crystallite size decreased at 3 GPa until 1100 °C, and then the crystallite size increased with increases in temperature >1100 °C. Similar trends were reported in the literature with field-assisted sintering processes. The effect of this too high temperature induces the growing of crystallites usually observed in the materials. In such a temperature domain, pressure cannot hinder the effect of temperature.

It can be observed that high pressure was necessary to obtain highly dense MgB_2 ceramics. However, thermal decomposition was initiated at 1150 °C under 3 GPa, and thermal decomposition occurred at 1300 °C under 5 GPa, as shown in the Figure 1. The characterization analyses of the MgB_2 ceramics sintered at different sintering conditions are discussed below.

Figure 2a shows the density of the sintered MgB_2 ceramics increased with the increase in pressure at a constant temperature of 950 °C. Pressure plays a pivotal role in significantly increasing the density of the sintered MgB_2 samples in the temperature domain where no decomposition occurs. The applied pressure of 5 GPa allows one to reach a fully dense MgB_2 ceramic, even at 950 °C, without thermal decomposition. This was impossible to reach by conventional SPS at 100 MPa, which resulted in only 90% density. However, pressure and temperature are interdependent on each other, as can be inferred from Figure 2b. It can be observed that temperature increased the density of the sintered sample at 3 GPa. There was a threshold limit for the temperature in the presence of pressure that led to an increase in relative density, and then the relative density decreased when thermal decomposition occurred, even in the presence of pressure. We can observe that HP-SPS at 3 GPa, even at 800 °C, was better than that at 950 °C and 100 MPa by conventional SPS, showing the real benefit of high pressure. We can observe that the presence of pressure during sintering at high temperature shifted the

thermal decomposition to a higher temperature at high pressure. The red hollow symbols in Figure 2b correspond to the thermal decomposition as observed by XRD at 100 MPa, 3 GPa, and 5 GPa.

**Table 1.** Calculation of crystallite size by the Scherrer equation.

Pressure	Temperature	Crystallite Size (nm)
50 MPa	950 °C	70
100 MPa	950 °C	73
100 MPa	1050 °C	91
100 MPa	1100 °C	104
1.7 GPa	950 °C	59
3 GPa	800 °C	67
3 GPa	950 °C	46
3 GPa	1100 °C	55
3 GPa	1150 °C	116
3 GPa	1200 °C	126
3 GPa	1300 °C	141
5 GPa	950 °C	44
5 GPa	1150 °C	75
5 GPa	1200 °C	68
5 GPa	1300 °C	131
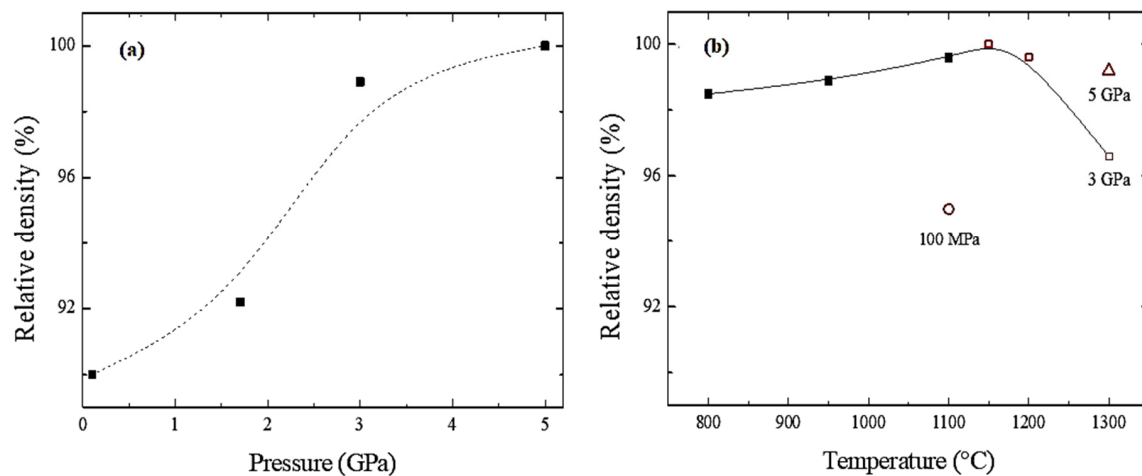
Figure 2. Density of MgB_2 with (**a**) Pressure at 950 °C and (**b**) Temperature at 3 GPa (red hollow symbols stand for decomposed samples).

3.2. Microstructural Analyses of MgB_2 Sintered Compacts

Figure 3 shows microstructures of the MgB_2 ceramics sintered by conventional SPS and high-pressure SPS. The density of the samples increased with the increase in temperature and pressure. It can be observed from Figure 3a,b that the samples sintered at 950 °C at 50 MPa and 100 MPa showed poorly connected microstructures containing a significant volume fraction of pores. In contrast, the sample processed at 800 °C at 3 GPa by HP-SPS in Figure 3c showed a homogenous microstructure and was relatively denser than the samples sintered by conventional SPS. With the increase in pressure, it can be observed that the sintered sample had a very dense microstructure and had no porosity. A large reduction in porosity with increasing pressure, in Figure 3d, was in good agreement with the density measurements presented in Figure 1.
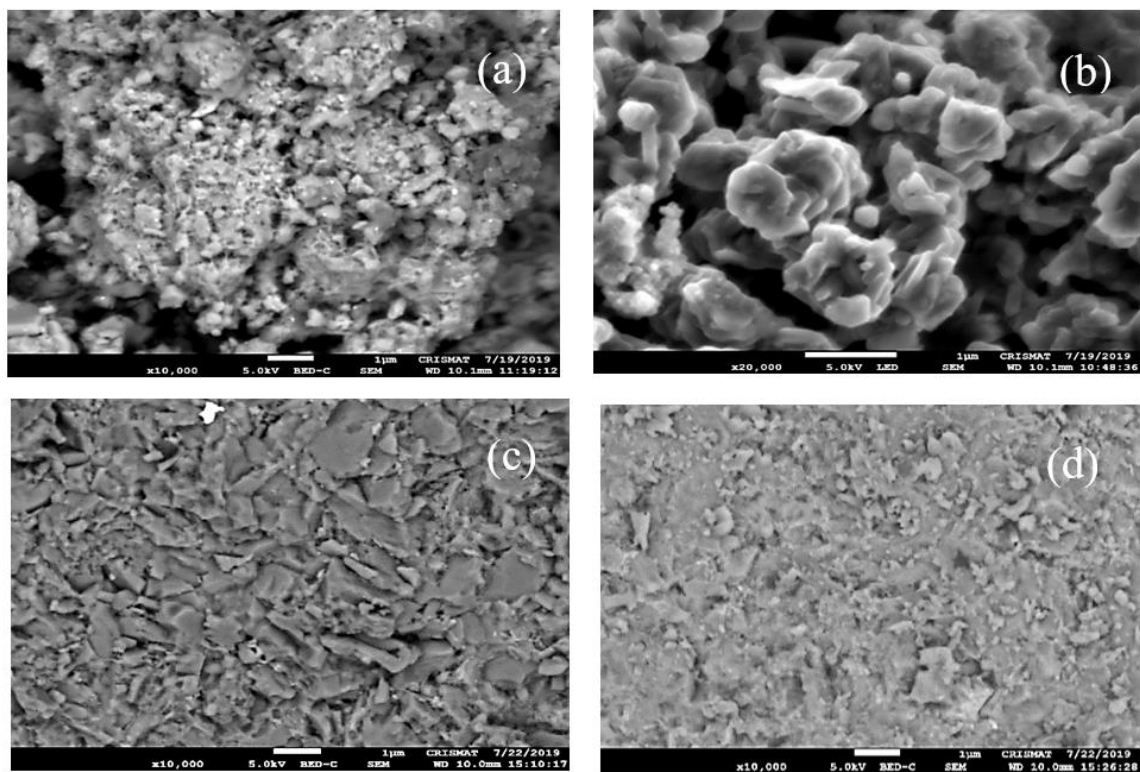
Figure 3. Microstructural evolution of sintered ceramics by conventional SPS at 950 °C at (**a**) 50 MPa, (**b**) 100 MPa, and by HP-SPS at (**c**) 800 °C, 3 GPa and (**d**) 950 °C, 5 GPa.

MgB_4 and MgO phases were observed at higher temperatures and lower pressures, indicating their thermal decomposition. Under high pressure, thermal decomposition was shifted to higher temperature, which was also ascertained with EDS studies indicating the percentage of MgO and MgB_4 phases formed at different temperatures and pressure. The atomic percentages of B, Mg, and O at 950 °C at 100 MPa and 3 GPa were as follows: B, 73.7; O, 2.9; Mg, 23.4; and B, 66.1; O, 9.3; Mg, 24.7, respectively.

3.3. Vickers Microhardness Analyses

The hardness of the samples was measured using Vickers indentation, and the average hardness for each sample is given in Table 2. The hardness was measured on 10 independent samples to obtain an average value of hardness. The ceramics obtained by conventional SPS for 950 °C at 50 MPa and 100 MPa were too fragile; hence, it was difficult to measure their hardness values, and no pellets were obtained by compression (by CIP at 200 MPa, by HP-SPS at 3 and 5 GPa) under ambient temperature. It can be observed that with the increase in pressure, the hardness increased, indicating a fine and homogenous microstructure as observed in SEM analyses.

Influence of pressure at low temperature (below 950 °C): Mechanical hardness was higher at 3 GPa and 800 °C than at 1.7 GPa and 950 °C, indicating the beneficial effect of pressure even at lower temperature (800 °C instead of 950 °C). Considering the error factor, the mechanical hardness requires further detailed analyses. In the aforesaid samples, however, XRD showed no decomposition of MgB_2. A similar trend for the increase in mechanical hardness was observed when the pressure increased from 1.7 to 5 GPa from 950 to 1200 °C. It can be inferred that the hardness value remained more or less stable (considering the error value) until 1300 °C. Later, at 1300 °C with decomposition of MgB_2, the hardness values showed a significant decrease.

Influence of temperature at high pressure: For instance, at 5 GPa the mechanical hardness increased up to 1200 °C and then decreased at 1300 °C. This correlates with the decomposition, which occurred at

1300 °C, as shown in XRD, although the variation of density was not significant. Mechanical hardness obtained at 3 GPa and 1100 °C was lower than expected because XRD did not show the decomposition of MgB_2, likely because the thermal stability of MgB_2 was just around 1100 °C and was not detectable by XRD. At 3 GPa, mechanical hardness decreased continuously with the increase in temperature from 1100 °C, probably as the decomposition increased.

Table 2. Measurement of Vickers microhardness for sintered MgB_2 ceramics.

Pressure (GPa)	Temperature (°C)	Density (g/cm^3)	Hardness (HV)
0.05 (SPS)	950	2.14 ± 0.01	Not measurable
0.1 (SPS)	950	2.37 ± 0.01	Not measurable
1.7 (HP-SPS)	950	2.59 ± 0.01	1347 ± 85
3 (HP-SPS)	950	2.57 ± 0.01	1404 ± 37
3 (HP-SPS)	1100	2.60 ± 0.01	1058 ± 88
3 (HP-SPS)	1150	2.61 ± 0.01	1039 ± 62
5 (HP-SPS)	950	2.62 ± 0.01	1465 ± 38
5 (HP-SPS)	1150	2.62 ± 0.01	1418 ± 51
5 (HP-SPS)	1200	2.62 ± 0.01	1460 ± 80
5 (HP-SPS)	1300	2.59 ± 0.01	1072 ± 80

Influence of pressure at high temperature (1150 °C): At this temperature, MgB_2 decomposed under ambient pressure (decomposition occurred around 650 °C), even at 100 MPa (decomposition occurred around 1050 °C by conventional SPS). Whereas, when the pressure was at 3 GPa, decomposition occurred at 1150 °C and was shifted to 1300 °C at 5 GPa, which was also clearly evident from the decrease in mechanical hardness correlated with variation in density

By following a similar trend as in structural ceramics, the hardness increased with increase in pressure and temperature. In the presence of high pressure and with the increase in temperature, the hardness increased in the thermal stability domain of MgB_2. On the other hand, it was evident that when the decomposition increased at high temperature in the presence of high pressure, this led to a decrease in density, which was in coherence with the density and corresponding microstructure. In the present work, we obtained high hardness values with the help of high pressure, which are higher than the reported hardness of MgB_2 in the literature [3] obtained by other sintering techniques. Ma et al. [19] reported to have obtained a high mechanical hardness (4109 HV) with high-pressure experiments by cubic anvil cells enclosed in molybdenum capsules at 5.5 GPa, 800 °C for 8 h dwell time. In the present work, we were able to achieve a high density and high hardness within 5 min of dwell time. The high hardness in the case of Ma et al. [19] can be attributed to a longer dwell time in comparison to the present work. In terms of industrial applications, the possibility of sample sizing to large dimensions and the total time taken for production are also vital to take into consideration. The influence of dwell time with our apparatus on yielding high mechanical hardness is currently under investigation.

3.4. Resistance Analyses

Figure 4 shows the temperature and pressure dependence of MgB_2 resistivity. The superconducting properties of MgB_2 are highly dependent on the density of the ceramic processed as well as on the grain boundaries acting as pinning sites [19,20] for large magnetic moments.
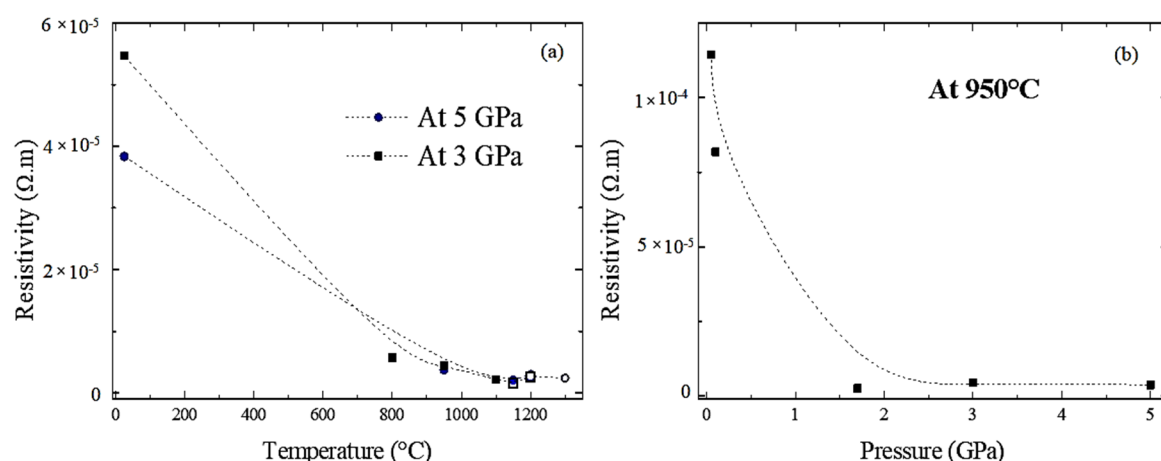
Figure 4. Resistivity of MgB_2 as a function of (**a**) temperature at 3 and 5 GPa and (**b**) pressure at 950 °C.

One would expect that, provided the materials were the same, dense samples would appear to have lower resistivity than porous samples, as the resistivity was calculated from the resistance and sample dimensions reported by those who made samples at lower pressures, and the effective cross-sectional area was smaller than the measured one (because the material does not fill the whole space). Figure 4a shows the benefit of identical temperature for 3 and 5 GPa where a threshold of resistivity appeared from 950 °C. The benefit of pressure in Figure 4b at 1.7 GPa probably derived from the high-density ceramics that were reached in this range of pressure. Resistivity values decreased systematically with increasing processing temperature, suggesting the MgB_2 lattice contains fewer defects and likely results in the superconductor having no parasitic phases [20,21]. Up to now, the majority of dense samples have been made by high-temperature and high-pressure (HT-HP) processes. It can be observed that with increasing pressure, the resistivity decreased in MgB_2 ceramics. The presence of Mg in the specimen has a significant role on influencing the resistivity, though the resistivity of magnesium was lower than the resistivity of MgB_2, and it decreased the overall resistivity. At high temperatures as well, we can observe that high pressure leads to a rapid decrease in resistivity. This was in accordance with the density and microstructural studies reported in this work, in addition to the beneficial effect of pressure on restricting the appearance of parasitic phases.

4. Conclusions

Highly dense MgB_2 polycrystalline samples were prepared by an in-house built ultrahigh pressure HP-SPS, and the systematically varied pressure and temperature were studied in order to analyze the effect of these variables on the final microstructure and superconducting properties. MgB_2 fully dense ceramics were obtained by maintaining the microstructured grains and by stabilizing the initial MgB_2 phases. High pressure inhibited the appearance of parasitic phases such as MgO and MgB_4, which occur due to thermal decomposition, by employing the beneficial effects of a field-assisted sintering DC pulse current associated with high pressure at temperatures above the thermal decomposition of MgB_2. These results indicate the importance of applied pressure in the production of dense magnesium diboride ceramics. This study investigated the role of high pressure in obtaining MgB_2 dense ceramics at temperatures below the thermal instability that occurs at high temperatures. The use of pressure strengthens covalent bonds [22] to increase the thermal stability domain of MgB_2 and, hence, allows one to sinter at temperatures higher than the thermal decomposition occurring at ambient pressure. This benefit of ultrahigh pressure applied by HP-SPS could be used for manufacturing highly dense ceramics, which present low decomposition temperatures or low melting temperatures. This work demonstrates that pressure acts like driving force. The superconducting properties of these highly dense MgB_2 ceramics are still being investigated and will be reported elsewhere in the near future.

References

1. Nagamatsu, J.; Nakagawa, N. Superconductivity at 39 K in magnesium diboride. *Nature* **2001**, *410*, 2–3. [CrossRef] [PubMed]

2. Buzea, C.; Yamashita, T. Review of superconducting properties of MgB2. *Supercond. Sci. Technol.* **2001**, *14*, R115–R146. [CrossRef]

3. Dancer, C.E.J.; Prabhakaran, D.; Başoğlu, M.; Yanmaz, E.; Yan, H.; Reece, M.; Todd, R.I.; Grovenor, C.R.M. Fabrication and properties of dense ex situ magnesium diboride bulk material synthesized using spark plasma sintering. *Supercond. Sci. Technol.* **2009**, *22*, 095003. [CrossRef]

4. Lee, S.Y.; Yoo, S.I.; Kim, Y.W.; Hwang, N.M.; Kim, D.Y. Preparation of dense MgB2 bulk superconductors by spark plasma sintering. *J. Am. Ceram. Soc.* **2003**, *86*, 1800–1802. [CrossRef]

5. Shim, S.H.; Shim, K.B.; Yoon, J.W. Superconducting characteristics of polycrystalline magnesium diboride ceramics fabricated by a spark plasma sintering technique. *J. Am. Ceram. Soc.* **2005**, *88*, 858–861. [CrossRef]

6. Yamamoto, A.; Tanaka, H.; Shimoyama, J.; Ogino, H.; Kishio, K.; Matsushita, T. Towards the Realization of Higher Connectivity in MgB2 Conductors: In-situ or Sintered Ex-situ? *Jpn. J. Appl. Phys.* **2012**, *51*, 010105. [CrossRef]

7. Viznichenko, R.V.; Kordyuk, A.A.; Fuchs, G.; Nenkov, K.; Müller, K.-H.; Prikhna, T.A.; Gawalek, W. Temperature dependence of trapped magnetic field in MgB2 bulk superconductor. *Appl. Phys. Lett.* **2003**, *83*, 4360–4362. [CrossRef]

8. Aldica, G.; Burdusel, M.; Popa, S.; Enculescu, M.; Pasuk, I.; Badica, P. The influence of heating rate on superconducting characteristics of MgB2 obtained by spark plasma sintering technique. *Phys. C* **2015**, *519*, 184–193. [CrossRef]

9. Aldica, G.; Popa, S.; Enculescu, M.; Pasuk, I.; Ionescu, A.M.; Badica, P. Dwell time influence on spark plasmasintered MgB2. *J. Supercond. Novel Magn.* **2018**, *31*, 317–342. [CrossRef]

10. Takano, Y.; Takeya, H.; Fujii, H.; Kumakura, H.; Hatano, T.; Togano, K.; Kito, H.; Ihara, H. Superconducting properties of MgB2 bulk materials prepared by high-pressure sintering. *Appl. Phys. Lett.* **2001**, *78*, 2914–2920. [CrossRef]

11. Häßler, W.; Scheiter, J.; Hädrich, P.; Kauffmann-Wei, S.; Holzapfel, B.; Oomen, M.; Nielsch, K. Properties of ex-situ MgB2 bulk samples prepared by uniaxial hot pressing and spark plasma sintering. *Phys. C* **2018**, *551*, 48–54. [CrossRef]

12. Krinitsina, T.P.; Kuznetsova, E.I.; Blinova, Y.V.; Degtyarev, M.V. Microstructure and critical current of bulk MgB2 superconductor. *J. Phys. Conf. Ser.* **2019**, *1389*, 012068. [CrossRef]

13. Prakasam, M.; Balima, F.; Cygan, S.; Klimczyk, P.; Jaworska, L.; Largeteau, A. Chapter 9-Ultrahigh pressure SPS (HP-SPS) as new syntheses and exploration tool in materials science. In *Spark Plasma Sintering*; Giacomo, C., Claude, E., Javier, G., Roberto, O., Eds.; Elsevier: Amsterdam, The Netherlands, 2019; pp. 201–218. [CrossRef]

14. Balima, F.; Bellin, F.; Michau, D.; Viraphong, O.; Poulon-Quintin, A.; Chung, U.-C.; Dourfaye, A.; Largeteau, A. High pressure pulsed electric current activated equipment (HP-SPS) for material processing. *Mater. Des.* **2018**, *139*, 541–548. [CrossRef]

15. Balima, F.; Largeteau, A. Phase transformation of alumina induced by high pressure spark plasma sintering (HP-SPS). *Scr. Mater.* **2019**, *158*, 20–23. [CrossRef]

16. Largeteau, A.; Prakasam, M. Trends in high pressure developments for new perspectives. *Solid State Sci.* **2018**, *80*, 141–146. [CrossRef]

17. Cannon, J.F. Behavior of elements at high pressure. *J. Phys. Chem. Data* **1974**, *3*, 781–825. [CrossRef]

18. Collings, E.W.; Sumption, M.D.; Bhatia, M.; Susner, M.A.; Bohnenstiehl, S.D. Prospects for improving the intrinsic and extrinsic properties of magnesium diboride superconducting strands. *Supercond. Sci. Technol.* **2008**, *21*, 103001–103057. [CrossRef]

19. Ma, H.A.; Jia, X.P.; Chen, L.X.; Zhu, P.W.; Ren, G.Z.; Guo, W.L.; Fu, X.Q.; Zou, G.T.; Ren, Z.A.; Che, G.C.; et al. Superhard MgB2 bulk material prepared by high-pressure sintering. *J. Phys. Condens. Matter* **2002**, *14*, 11181–11184. [CrossRef]

20. Matthews, G.A.B.; Liu, J.; Grovenor, C.R.M.; Grant, P.S.; Speller, S. Design and characterisation of ex situ bulk MgB2 superconductors containing a nanoscale dispersion of artificial pinning centres. *Supercond. Sci. Technol.* **2020**, *33*, 034006. [CrossRef]

21. Matthews, G.A.B.; Santra, S.; Ma, R.; Grovenor, C.R.M.; Grant, P.S.; Speller, S.C. Effect of the sintering temperature on the microstructure and superconducting properties of MgB2 bulks manufactured by the field assisted sintering technique. *Supercond. Sci. Technol.* **2020**, *33*, 054003–054014. [CrossRef]

22. Demazeau, G. High Pressure and Chemical Bonding in Materials Chemistry. *Z. Nat.* **2006**, *61*, 799–808.